NIH Public Access
Author Manuscript
J Neural Eng. Author manuscript; available in PMC 2014 June 01.

Published in final edited form as:
J Neural Eng. 2013 June ; 10(3): 036020. doi:10.1088/1741-2560/10/3/036020.

Laminar stream of detergents for subcellular neurite damage in a microfluidic device: a simple tool for the study of neuroregeneration

Chang Young Lee[a,b], **Elena V. Romanova**[b], and **Jonathan V. Sweedler**[b,*]

[a]School of Nano-Bioscience and Chemical Engineering, Ulsan National Institute of Science and Technology (UNIST), Ulsan, 689-798, Korea

[b]Department of Chemistry and the Beckman Institute, University of Illinois, Urbana, IL 61801, USA

Abstract

The regeneration and repair of damaged neuronal networks is a difficult process to study *in vivo*, leading to the development of multiple *in vitro* models and techniques for studying nerve injury. Here we describe an approach for generating a well-defined subcellular neurite injury in a microfluidic device; a defined laminar stream of sodium dodecyl sulfate (SDS) was used to damage selected portions of neurites of individual neurons. The somata and neurites unaffected by the SDS stream remained viable, thereby enabling the study of neuronal regeneration. The SDS transection approach is simple and inexpensive, yet provides flexibility in studying neuroregeneration, particularly when it is important to make sure there are no retrograde signals from the distal segments affecting regeneration. By using well-characterized neurons from *Aplysia californica* cultured *in vitro*, we demonstrate that our approach is useful in creating neurite damage, investigating neurotrophic factors, and monitoring somata migration during regeneration. Supplementing the culture medium with acetylcholinesterase (AChE) or *Aplysia* hemolymph facilitated the regeneration of the peptidergic *Aplysia* neurons within 72 h, with longer ($p < 0.05$) and more branched ($p < 0.05$) neurites than in the control medium. After the neurons were transected, their somata migrated; intriguingly, for the control cultures, the migration direction was always away from the injury site (7/7). In the supplemented cultures, the number decreased to 6/8 in AChE and 4/8 in hemolymph, with reduced migration distances in both cases. Neurons are known to not only be under tension but also balanced in terms of force, and the balance is obviously disrupted by transection. Our experimental platform, verified with *Aplysia*, can be extended to mammalian systems, and help us gain insight into the role that neurotrophic factors and mechanical tension play during neuronal regeneration.

Introduction

Understanding the processes involved in neuronal regeneration is integral to advancing our ability to treat nervous system injuries and neurodegenerative diseases. Having an analytical platform that can reliably culture, damage, and monitor individual neurons during their regeneration helps further this goal. Microfluidic devices can not only handle small liquid

*Corresponding author: Jonathan V. Sweedler, Tel: 217.244.7359, Fax: 217.265.6290, jsweedle@illinois.edu.

Classification Scheme: PACS
87.19.L- Neuroscience
87.85.dh Cells on a chip, in applied neuroscience
47.15.-x Fluid flow, laminar

NIH-PA Author Manuscript
NIH-PA Author Manuscript
NIH-PA Author Manuscript

NIH-PA Author Manuscript

NIH-PA Author Manuscript

NIH-PA Author Manuscript

volumes, but they also offer the option of automated operation while potentially mimicking an extracellular microenvironment at high spatiotemporal resolutions [1, 2]. These systems have therefore shown great promise in biological research, including neuroscience, and more specifically, in the study of regeneration. Previous studies have demonstrated reliable neuronal cultures within the microchannel [3], often on pre-selected regions via chemical [4] or topographical [2, 5] guidance. As an entire microfluidic system can be made optically transparent, neurons in the device can be characterized by well-established procedures such as immunohistochemistry followed by microscopic observations [2, 3]. Electrophysiological measurements, both intracellular [6, 7] and extracellular [8], can be performed, although the additional fabrication steps required make these approaches less versatile at present. The ability to handle mass-limited samples with minimal loss or dilution has been helpful in the delivery of stimulants through artificial synapses [9], or collection of the neuronal signaling molecules and subsequent analysis with mass spectrometry [10, 11].

Most regeneration studies have involved physical or optical damage such as ablation with pulsed lasers [12], severing with a micropipette [13, 14], microneedle [15], or nanoknife [16], and crushing with microfluidic compression [17]. These approaches have a number of advantages but often require elaborate experimental setups or expertise in optics and microfabrication, and thus are not readily available to the broader neuroscience community. Several studies have used a three-compartment microfluidic device to remove axons in the central compartment either by vacuum aspiration [2] or by introducing a saponin solution [18]. These are elegant approaches but lack flexibility in determining the location and width of the damage, and are not practical in low-density cultures due to the poor yield of neurites that bridge multiple compartments.

The study of regeneration will be well served both by new tools and a well-defined model system that is easy to maintain, observe, and measure in culture within a microfluidic device. Here we worked with the relatively large and well-characterized neurons of the marine mollusk *Aplysia californica*, which have been used for a number of studies involving morphology and function on well-defined surfaces [19-21]. *Aplysia* neurons are known to morphologically and functionally regenerate *in vitro* by re-forming synaptic connections after transection, and have previously served as a model for regeneration studies [14, 22, 23]. Several researchers have studied the post-transection responses, which typically include hyperexcitability and hypermorphogenesis [24, 25]. Transection without *Aplysia* hemolymph in the culture medium induces hyperexcitability but not hypermorphogenesis [26]. When the severed distal segment is not removed and remains close to the proximal counterpart, the two reconnect, in which case both post-transection responses are suppressed [15]. These results suggest that the long-term post-transection responses are at least partially intrinsic and associated with retrograde signals from the remaining distal segment [15]. We also suspect effects of retrograde signals from the damaged but remaining *proximal* segment. Hence, a transection tool that removes the distal segment completely will help us distinguish retrograde signaling both from proximal and distal neurites during regeneration. Efforts have been made to facilitate the regeneration of *Aplysia* neurons by adding neurotrophic factors. Among the effective factors that have been used are serotonin [27, 28], *Aplysia* β-thymosins [29, 30], acetylcholinesterase (AChE) [31], and *Aplysia* hemolymph [32]. Nonetheless, many details of the regeneration process remain unclear.

Here we describe a laminar flow-based microfluidic technique for chemically damaging neurites at subcellular resolution; the approach can be used as a tool for studying neuronal regeneration and motility. The liquid flow in a microchannel is laminar, due to a large viscous force or small Reynolds number (*Re*, ratio of inertial force to viscous force). In this flow regime, multiple streams can flow side-by-side, with mixing occurring by diffusion. Multiple laminar streams allow delivery of the chemicals of interest to a selected region in

NIH-PA Author Manuscript

NIH-PA Author Manuscript

NIH-PA Author Manuscript

the channel. Examples of this focal delivery include: protein patterns on a substrate for cellular adhesion [33], stimulation of a plant root for local GFP expression [34], subcellular delivery of small molecules [35], localized trypsin to detach a cell population [36, 37] or a subcellular domain [38], and localized migration assays to either promote or inhibit cellular migration [37]. Laminar flow allows precise subcellular delivery of cytotoxic compounds without directly affecting the unexposed cellular domain.

In our approach, a stream of sodium dodecyl sulfate (SDS) was applied in order to remove a selected portion of neurites in *Aplysia* bag cell neurons in the microchannel. The damaged neurons remained viable and continued to extend their neurites. We found that supplementing the culture medium with AChE or *Aplysia* hemolymph significantly enhanced neurite regeneration while suppressing the migration of soma. By implementing this chemical transection technique, we gained insight into the role that neurotrophic factors and mechanical tension play during neuronal regeneration. Compared with previous transection methods, ours is simple and inexpensive, and does not require elaborate pulsed-laser setups or additional microfabrication steps. The distal segments, and thus the retrograde signals from these segments, are removed by the detergent stream. The approach also provides flexibility as the region to be transected can be determined on demand by varying the ratio of flow rates. In summary, the transection method presented here will serve as a complementary tool for neuroregeneration research.

Experimental

Chemicals and reagents

Chemicals were purchased from Sigma Aldrich (St. Louis, MO) unless specified otherwise. Artificial seawater (ASW), pH 7.8, was prepared with 460 mM NaCl, 10 mM KCl, 10 mM $CaCl_2$, 22 mM $MgCl_2$, 26 mM $MgSO_4$, 15 mM HEPES, 2.5 mM $NaHCO_3$ and supplemented with antibiotics for cell culture. AChE from *Electrophorus electricus* (electric eel) was purchased from Sigma Aldrich. *Aplysia* hemolymph was collected from an adult animal (80 g), filtered with 0.22 μm pore filters (Millipore, Billerica, MA), kept frozen at −20 °C, and mixed with ASW at a 50/50 ratio right before use. ASW and *Aplysi*a hemolymph have similar osmolarity [39], and thus the reported results are not affected by differences in osmolarity.

Microfluidic device fabrication

We adopted the design and fabrication methods of our polydimethylsiloxane (PDMS) microfluidic device from Tourovskaia et al. [1, 40], with modifications. Briefly, a master was created by patterning SU-8 negative photoresist (MicroChem, Newton, MA) on a silicon substrate (WRS Materials, San Jose, CA) via standard photolithography. Fluidic connections were made by gluing (Duco Cement, Devcon, Danvers, MA) silicone tubing (Helix Medical, Carpinteria, CA) onto ports 2, 3, and 5 of the master mold (figure 1A), followed by pouring PDMS prepolymer (Sylgard 184, Dow Corning, Midland, MI) and curing at 70 °C overnight. The PDMS structure was then peeled off and sealed onto a tissue culture dish (CELLSTAR, Greiner Bio-One, Monroe, NC) by conformal contact. A cut-out pipette tip was glued onto port 4 with PDMS prepolymer, followed by another curing session. Finally, the device was filled with ASW for cell culture by applying a vacuum to ports 2, 3, and 5 while ports 1 and 4 were filled with ASW.

Cell culture and loading into device

Adult *Aplysia californica* (National Resource for *Aplysia*, Miami, FL) weighing ~80 g were anesthetized by injecting ~½ body weight of $MgCl_2$ (0.39 M), and the abdominal ganglia dissected. After treating the ganglia with protease (from *Streptomyces griseus*, 10 mg/mL in

NIH-PA Author Manuscript

NIH-PA Author Manuscript

NIH-PA Author Manuscript

ASW) for 100 min at 34 °C to soften the surrounding tissue, bag cell neurons were isolated from the bag cell clusters near the pleurovisceral connectives. For cell culture in the microfluidic devices, cells were loaded into the main channel (< 5 cells/device) by dropping them into port 1 while applying vacuum at either port 2 or 3. We were able to roughly control the location of the plated cells by inspecting the channel under a microscope while loading, and releasing the vacuum when desired. The device was then perfused with ASW (~20 μL/d) by elevating the ASW level in the pipette tip at port 4. Ports 1-3 were closed so that the perfusion took place from port 4 to 5. The cultures were maintained at 14 °C. Although the cellular responses we describe were qualitatively consistent in multiple animals, quantitative comparisons were made across cells from the same animal to prevent any ambiguity due to animal-to-animal variation (see Results and Discussion).

Neurite transection

In order to dissolve the cell membrane, a detergent solution was prepared by mixing at a 1:1 ratio, 20 mM of SDS and 10 mM of Allura Red dye in ASW. The dye helps to visualize the stream and adjust the flow rates when necessary. Neurites of bag cell neurons at 3 d *in* vitro (DIV) were partially damaged by introducing laminar flows of the SDS solution and ASW at ports 2 and 3, as shown in figure 2A. Using syringe pumps (PHD 2000, Harvard Apparatus, Holliston, MA) the SDS:ASW flow rates were varied between 0.5:4.5 μL/min and 0.5:9.5 μL/min, depending on the location and morphology of the cell. Since the SDS stream damages the cells along the path, in some devices we were able to transect multiple cells (up to 4 cells per device) in a single operation. Immediately after the membrane damage, which is normally observed within 3 min of the flow initiation, the channel was flushed with ASW at 10 μL/min for at least 3 min to remove any residual SDS. Finally, the device was perfused with ASW only, ASW with AChE (5 U/mL), or ASW with 50% *Aplysia* hemolymph.

Microscopy and morphometry

Neuron images were obtained with an Axiovert 25 inverted microscope (Zeiss, Zena, Germany) with phase contrast optics. The neurites were traced in Neurolucida software (MBF Bioscience, Williston, VT), and the changes of length and branch structures during regeneration were analyzed in Neurolucida Explorer (MBF Bioscience).

Results and discussion

Culture of Aplysia neurons in a microfluidic device

The study of neuronal damage and subsequent regeneration in a microchannel requires maintaining a reliable neuronal culture during the course of regeneration; when one works with only a single cell (or perhaps several cells) at a time, even stricter limits on reliability are required. For this purpose, we adopted and slightly modified the design from Tourovskaia et al. [1, 40] used for long-term studies of muscle cell differentiation. Our device, shown in figure 1A, consists of a main channel for cell culture, side channels for perfusion of culture medium, and ports (labeled 1–5) for cell loading and fluidic connections. The main channel (W × H = 500 μm × 250 μm) is large enough to accommodate the *Aplysia* bag cell neurons (diameter ~50 μm) used in this study. Bag cell neurons, which are involved in egg laying behavior of the animal [41], are abundant (~400–800 cells/animal), easy to isolate, and appear homogeneous [42], and thus, enable cell-to-cell comparative studies while ruling out animal-to-animal variation. Figure 1B shows a bag cell neuron cultured in the device filled and perfused with ASW at 1 DIV (top) and 3 DIV (bottom). Neurites continued to extend their length with more branches and the cells remained viable for more than 2 wk. The cell viability observed in our device was over 50% and did not depend on the location at which the cell was seeded in the channel. This

NIH-PA Author Manuscript

NIH-PA Author Manuscript

NIH-PA Author Manuscript

platform provided several advantages for the current study: with the large neurons of *Aplysia*, single-cell experiments were conducted with high yield; laminar flow through ports 2 and 3 allowed focal delivery of chemical compounds to a selected subcellular domain; and culture medium supplied from port 4 was easily supplemented with factors of interest to study cellular responses.

We were able to reliably culture *Aplysia* bag cell neurons in a PDMS microchannel without further conditioning or surface modifications of the PDMS. Treating the PDMS with an oxygen plasma is a standard procedure in soft lithography in order to enhance the hydrophilicity of the material and facilitate bonding to a substrate [43]. However, the oxygen permeability in PDMS decreases ~1000 fold when treated with oxygen plasma or bovine serum albumin [44]. In our study, using a native PDMS and culturing only a few cells per device is beneficial in terms of ensuring adequate oxygen supply. Another consideration is to minimize protein adsorption/absorption by the PDMS, as well as the cytotoxicity of residual metal catalysts, solvents, and uncrosslinked oligomers [3, 45, 46]. Previous studies have shown that appropriate treatments of the PDMS, such as autoclaving [1, 3], solvent extraction [3, 47], or functionalization with polyethylene glycol [48], help address these issues, especially for a low-density culture of mammalian neurons [3]. In this respect, using native PDMS perhaps creates a problem.

Performing a quick calculation further clarifies this issue and demonstrates that culturing the larger *Aplysia* neurons we used takes careful optimization of culturing conditions. A relevant dimensionless quantity related to the leaching of compounds from the device is derived from the Sherwood number, $Sh = kL/D$, and Peclet number, $Pe = vL/D$, where k, L, v, and D denote mass transfer coefficient, characteristic length, fluid velocity, and diffusivity, respectively. *Sh* indicates the ratio of the mass transfer rate at the PDMS surface to the diffusion rate in the media [49]. *Pe* is the ratio of the convection rate to the diffusion rate in the media. A large Sh/Pe (= k/v) for the potentially cytotoxic molecules leaching out of PDMS could reduce the cell viability. While k is unknown, the perfusion rate of 20 μL/d turns out to be sufficient for a small Sh/Pe. At the higher perfusion rates tested here (150–300 μL/d), the Sh/Pe term is further reduced; however, both the viability and the growth rate dropped significantly, perhaps due to excessive shear stress. Interestingly, for smaller cells plated at high density, the optimal perfusion rate can be much higher, even with a similar device design [1, 50, 51]. Hence, a low-density culture of large neurons requires a carefully optimized perfusion rate at which appropriately low levels of cytotoxicity and minimal shear stress are achieved. This challenge may explain why there are few examples of *Aplysia* neurons cultured in a microfluidic device.

Damage of neurites via a laminar stream of detergent

A single-neuron microfluidic device allows us to make subcellular chemical modifications via laminar flow. Previously Takayama et al. [35] utilized a laminar stream for subcellular delivery of trypsin for partial cell *detachment*, followed by *re-attachment* upon removal of the trypsin [38]. The timescale for the cell detachment was on the order of minutes. In the current study we applied a focal delivery of SDS, an anionic detergent, to *damage* (or completely remove) neurites of a single neuron from a selected subcellular domain. Because laminar flow is a physical process, with appropriate modifications of the flow rate and culture media, our chemical transection approach should be applicable to a wide variety of cells including mammalian neurons. Here we chose to test the approach with *Aplysia* neurons because of the robustness of their culture, the ability to work with defined neuronal subtypes from primary cultures, and the detail available on their response to axotomy [23-27].

NIH-PA Author Manuscript

NIH-PA Author Manuscript

NIH-PA Author Manuscript

The schematics in figure 2A illustrate the approach, where two laminar streams, SDS on the left and ASW on the right, flow over a single neuron to cause localized damage. A bag cell neuron is shown in figure 2B, before (top) and after (bottom) such an operation. Only the cell membranes on the left-hand side were removed, while the soma and the unexposed neurites on the right-hand side remained intact. The width of transection can be controlled from 0 to the entire channel width of 500 μm by varying the ratio of SDS-to-media flow rates. However, there is an additional undesired neurite damage region due to molecular diffusion in the direction perpendicular to the flow. The width of undesired damage scales ~ $2(Dt)^{0.5}$ where D and t represent diffusivity and time, respectively. At 10 μL/min and D = 6 × 10^{-7} cm^2/s [52] this becomes ~ $0.424y^{0.5}$ μm where y (in μm) is the distance down the channel from the inlet. When the SDS stream encounters the neurite, there may be further damage by migration of SDS along the neurite. Figure 2C shows a series of time-lapse images of the membrane being removed. The membrane damage occurred within seconds of contact with the SDS. As seen in the upper portion of the figure, the membrane damage became broader over time due to the migration of the SDS molecules along the neurite toward the cell body. Therefore, a precise spatiotemporal control of the flow minimizes undesired neurite or membrane damage.

Detergents have been widely used in biological research to either solubilize or permeabilize the cell membrane for extraction of proteins and organelles, or for transfection, respectively [53]. The SDS used in our study is an anionic and strongly solubilizing detergent. The critical micelle concentration above which micelles are formed is 6–8 mM for SDS. Above the critical micelle concentration (10 mM in this study) a direct interaction between SDS micelles and the cell membrane quickly overpermeabilizes and disaggregates the membrane [54]. Although SDS tends to denature proteins, it served well our purpose of damaging the membrane. When non-denaturing detergents such as nonionic Triton × or zwitterionic CHAPS (3-[(3-cholamidopropyl)dimethylammonio]-1-propanesulfonate) are used, our approach may find further applications in extracting proteins and organelles from subcellular domains without sacrificing the neuron. Multiple extractions from the same neurite can even be made at distinct time points, assuming the cell regenerates. Our chemical transection approach is robust, simple and easy to implement.

Surprisingly, upon membrane damage the neurites did not show signs of an immediate retraction toward the cell body, which is distinct from several prior reports [12, 13]. Tension in the nervous system plays not only a functional role, such as in synaptic signaling [55] and vesicle trafficking [56], but also appears to have an important morphogenetic role in the formation of neural structures such as the cerebral and cerebellar cortexes [57]. Within a single neuron, neurites are known to be under tension, and the force vectors from neurites sum to zero ($\Sigma F = 0$) [58]. Mechanically or optically severing a neurite causes a force unbalance, followed by a retraction of the damaged neurite with either weak or disrupted neurite-substrate adhesion. This often leads to formation of rippled shrink patterns [13]. The localized chemical damage in this work is unique in that the detergent dissolves the membrane without applying a disturbing force, as in mechanical approaches that physically detach neurites from the substrate or affect global neurite-substrate interactions. Thus, the immediate responses to restore the balance (*e.g.,* shrinking) are thereby suppressed. Instead, the neuron goes through rather long-term changes such as restoring the force balance, discussed later.

Neurotrophic factors for regeneration of the damaged neurites

The ability to damage selected neurites of individual neurons, and control the extracellular chemical environment, facilitates the study of the roles that putative neurotrophic factors play in neurite regeneration. By following the response of the neuron to subcellular, chemically-induced damage, we can investigate the neurotrophic factors that enhance the

NIH-PA Author Manuscript

NIH-PA Author Manuscript

NIH-PA Author Manuscript

regeneration processes. We first examined neuronal growth on a culture dish with and without previously reported neurotrophic factors: serotonin [27, 28], nerve growth factor (NGF) [59], thymosin 4 (16-38) containing an actin-binding domain [29, 60], AChE [31], and the less chemically well-defined native *Aplysia* hemolymph [32]. Based on qualitative comparisons between the samples (figure S1, Supplementary Information), we selected AChE and hemolymph as intriguing candidates that enhance regeneration of the chemically damaged neurons in our microfluidic device. Neurons cultured in ASW for 3 d were transected with localized SDS streams, and just after the transection, the device was perfused with either ASW only (control, n = 7) or ASW supplemented with AChE (5 U/mL, n = 8) or hemolymph (50%, n = 8) where n represents the number of independent single-cell experiments. We monitored and compared the regeneration process for 3 d post-transection with primary attention to the neurite length, number of branch points, and location of the soma. Figure 3 shows representative images of neurons before/after neurite damage and at 24 h, 48 h, and 72 h post-transection under different culture media: ASW only (figure 3A), ASW with AChE (figure 3B), and ASW with hemolymph (figure 3C). Regions that are false-colored red in the “Before” column represent the laminar streams of SDS and the corresponding regions of neurite damage. In ASW only, the cell remained viable and the length of neurites increased overall. However, regeneration of the damaged neurite was sluggish. In contrast, the neurons in AChE and hemolymph regenerated their damaged neurites with generally longer and more branched neurites. Neurites grow into the area exposed to SDS, which verifies that SDS does not degrade the substrate during transection. No negative effect of SDS on cell viability and outgrowth was observed in a separate control experiment (figure S2, Supplementary Information).

We quantified the overall neurite structure of 23 transected neurons during regeneration. Keeping track of the transected neurites separately from the untransected ones was not practical; the number of primary neurites changed as transected neurites degenerated or merged with neighboring neurites. Hence, we chose not to track individual neurites in this analysis. Instead we show the total neurite growth (figure 4A) and the total number of new branch points (figure 4B), which include both transected and untransected neurites, that had been added since the time of transection (t = 0 h) in the different cell media. Even with the large morphological heterogeneity at the single cell level, within 6 h the neurons in hemolymph regenerated significantly ($p < 0.01$) and became more branched ($p < 0.05$) than the control. A linear fit for the entire period with a zero intercept gives the regeneration rates of 22 ± 1, 29 ± 1, and 42 ± 3 μm/h, and the increased rates of branch points of 6.8 ± 0.4, 9.1 ± 0.1, and 17 ± 2 branches/d for the control, AChE, and hemolymph samples, respectively. For the neurons in hemolymph, a straight line does not give the best fit as the initially fast growth rates diminished over time, presumably due to the limited space in the channel: 75, 50, 30, 32 μm/h and 44, 19, 12, 9 branches/d at 6, 24, 48, and 72 h, respectively.

AChE, an enzyme that catalyzes the hydrolysis of acetylcholine, is abundant in *Aplysia* hemolymph, along with other proteins such as hemocyanin and hemagglutinin [31, 61]. Other than the catalytic function, the high level of expressed AChE during extensive neurite outgrowth [31, 62] indicates its potential neurotrophic function. Indeed, AChE has been shown to help neurite regeneration of dopaminergic neurons of *Aplysia* via a non-catalytic mechanism [31]. Based on similarity searches, Srivatsan [63] hypothesized that the carboxylesterase type B region in AChE may act as a growth factor, but the mechanisms of the non-catalytic action of AChE are still unknown. The neurotrophic effects of *Aplysia* hemolymph, with its large amounts of AChE, on cholinergic neurons [64] and others [29, 32], suggest that AChE might also help the neurite growth of other types of *Aplysia* neurons. In this study we show that AChE, as well as *Aplysia* hemolymph, helps the regeneration of chemically damaged neurites of peptidergic *Aplysia* bag cell neurons. However, the effects of AChE alone develop more slowly and do not become significant ($p < 0.05$) until 72 h in

NIH-PA Author Manuscript

NIH-PA Author Manuscript

NIH-PA Author Manuscript

culture, while the effects of hemolymph are observed after only 6 h (figure 4). We believe that the amino acids and neurotrophic factors in hemolymph rather than AChE facilitate the faster neurite regeneration. Details on the regeneration process (*e.g.*, whether it is cholinergic or non-cholinergic) is largely unknown, and our single-neuron microfluidic system should help in answering these questions.

Tension during regeneration of neurites

The leading edges of growing neurites create growth cones that generate tension, which pulls the soma forward (towards the growth cone) and results in the coordinated motility of the cell soma and its extending neurites [65]. Upon transection of a neurite, not only can the neurite regenerate, as shown in figures 3 and 4, but tension by the remaining neurites is expected to pull the soma toward the direction of the intact neurites (*most* away from the injury site) as a part of long-term regenerative behavior. In figure 5A we have tracked the migration paths of soma for the transected bag cell neurons (n = 7, 8, and 8, for ASW, AChE, and hemolymph, respectively), starting from their location right after the transection (shown as black filled circles). Red and blue colors are used for cells with neurites cut on the left- and right-hand side of the soma, respectively. All cells (7/7 or 100%) cultured in ASW migrated away from the injury site, which can be explained in terms of tension as discussed above. However, the number decreased to 6/8 (75%) and 4/8 (50%) in AChE and hemolymph, respectively. Here the question arises as to whether or not the migration is a regenerative behavior. A separate experiment using another animal of the same species, which therefore cannot be directly compared with the results in figure 5, showed that neurons in our device did migrate (53 ± 8 μm at 72 h, n = 8), even without transection, when cultured in ASW. These results suggest that the regenerative behavior in ASW can be signified not by the migration itself, but by the direction of migration, which is systematically away from the transected neurites.

Further insight can be gained by quantifying the soma migration. The white bars in figure 5B indicate the x-component of the migration *away* from the injury site, and so the value is negative when migrating toward the injury. The smaller values in AChE and hemolymph ($p < 0.06$) than in ASW indicate that the migration direction is insensitive to which side of the soma is transected. The bar graph in figure 5B also shows the total migration distance over 72 h (black) and the linear displacement from 0 h to 72 h (gray). Even with large cell-to-cell variations, the post-transection neuronal migration is reduced significantly in AChE and hemolymph ($p < 0.06$), which potentially can be explained by earlier restoration of balancing tension and forces due to faster neurite regeneration, as shown in figure 4. We found that most of the post-transection morphological changes that presumably help restore the force balance can be described as a combination of the following: regeneration of neurites (i.e., added length and branch points), reorientation of neurites, and migration of soma. The results, shown in figures 4 and 5, suggest a correlation between the neurite regeneration and somata migration. We conclude that the modes of regaining the force balance during regeneration vary, depending on the extracellular chemical environment. Moreover, when neurotrophic factors are present, as they appear to be *in vivo*, the process occurs mainly via regeneration of neurites rather than cellular migration.

Cellular forces have been measured and controlled via techniques such as PDMS micropillars [66], stretchable PDMS platforms [56], vertical nanowire arrays [67], and axon-bound [68], substrate-embedded [69], or optically-trapped [70] beads. Our study shows a post-injury neuronal migration that is related to tension that can be further studied quantitatively by incorporating these techniques into our system.

NIH-PA Author Manuscript

NIH-PA Author Manuscript

NIH-PA Author Manuscript

Conclusions

Microfluidic systems have shown potential for studying neuronal regeneration at the single cell level because of their small volumes and well-controlled fluidics. However, the sealed channels require a new method to damage selected sections of a neuron in order to study the processes of neuronal regeneration. In this study we used two parallel laminar streams, SDS dissolved in cell media and media only, to transect a selected subcellular portion of an *Aplysia* bag cell neuron in a microfluidic channel. Our chemical transection approach, albeit simple, provides a unique opportunity to study neuronal regeneration where the severed segment and thus, the retrograde signals from it, are removed by the SDS. This type of damage is difficult to achieve with previously-reported pulsed lasers or microfluidic compression. Using this platform we were able to investigate the post-transection cellular responses. The results suggest that when appropriate neurotrophic factors are present, the neurons restore the force balance between neurites, which is broken by transection, primarily by neurite outgrowth rather than somata migration.

Future efforts include expanding these studies to examine the distal segments of severed processes by sandwiching the SDS stream between two ASW streams in order to further our understanding of the mechanisms of regeneration, and applying our approach to mammalian systems. Our technique creates subcellular damage. We will find more opportunities to increase our understanding of mammalian nerve regeneration as the challenges in maintaining a low-density mammalian culture are resolved. When combined with previously developed force sensors, our system should allow quantification of the cell responses and changes in force distributions during regeneration. Furthermore, the extracellular environment of the damaged and repairing cell can be collected for additional characterization; we have already demonstrated the ability to collect small-volume samples from neurons in a device for hormone and peptide characterization [71-73]. We will extend our studies to study regeneration of mammalian neurons and modify our readout to include both metabolomics responses via mass spectrometry [71, 74] and transcriptional responses to injury, for example, via single cell RNA amplification [75].

Supplementary Material

Refer to Web version on PubMed Central for supplementary material.

Acknowledgments

The authors thank Dr. Stanislav Rubakhin, Dr. Ming Zhong, and Callie Croushore for useful discussions, and Xiying Wang for assistance with animal dissection. We acknowledge the support of the National Science Foundation by Award No. DMI-0328162, the National Institute of Neurological Disease and Stroke by Award No. NS031609, and the National Institute on Drug Abuse by Award No. DA018310. This work was also supported by the National Research Foundation of Korea (NRF) grant funded by the Korea government (MEST) (No. 2012K1A3A1A09055096) and by the year of 2012 Research Fund of the UNIST (Ulsan National Institute of Science and Technology). *A. californica* were partially provided by the National Resource for *Aplysia* at the University of Miami under NIH National Center for Research Resources grant RR10294. The content is solely the responsibility of the authors and does not necessarily represent the official views of the awarding agencies.

References

[1]. Tourovskaia A, Figueroa-Masot X, Folch A. Long-term microfluidic cultures of myotube microarrays for high-throughput focal stimulation. Nat. Protoc. 2006; 1:1092–104. [PubMed: 17406389]

[2]. Park JW, Vahidi B, Taylor AM, Rhee SW, Jeon NL. Microfluidic culture platform for neuroscience research. Nat. Protoc. 2006; 1:2128–36. [PubMed: 17487204]

NIH-PA Author Manuscript NIH-PA Author Manuscript NIH-PA Author Manuscript

[3]. Millet LJ, Stewart ME, Sweedler JV, Nuzzo RG, Gillette MU. Microfluidic devices for culturing primary mammalian neurons at low densities. Lab Chip. 2007; 7:987–94. [PubMed: 17653340]

[4]. Rhee SW, Taylor AM, Tu CH, Cribbs DH, Cotman CW, Jeon NL. Patterned cell culture inside microfluidic devices. Lab Chip. 2005; 5:102–07. [PubMed: 15616747]

[5]. Rajnicek AM, Britland S, McCaig CD. Contact guidance of CNS neurites on grooved quartz: Influence of groove dimensions, neuronal age and cell type. J. Cell Sci. 1997; 110:2905–13. [PubMed: 9359873]

[6]. Ionescu-Zanetti C, Shaw RM, Seo JG, Jan YN, Jan LY, Lee LP. Mammalian electrophysiology on a microfluidic platform. Proc. Natl. Acad. Sci. U. S. A. 2005; 102:9112–17. [PubMed: 15967996]

[7]. Hsu CH, Chen CC, Folch A. “Microcanals” for micropipette access to single cells in microfluidic environments. Lab Chip. 2004; 4:420–24. [PubMed: 15472724]

[8]. Dworak BJ, Wheeler BC. Novel MEA platform with PDMS microtunnels enables the detection of action potential propagation from isolated axons in culture. Lab Chip. 2009; 9:404–10. [PubMed: 19156289]

[9]. Peterman MC, Noolandi J, Blumenkranz MS, Fishman HA. Localized chemical release from an artificial synapse chip. Proc. Natl. Acad. Sci. U. S. A. 2004; 101:9951–54. [PubMed: 15218102]

[10]. Jo K, Heien ML, Thompson LB, Zhong M, Nuzzo RG, Sweedler JV. Mass spectrometric imaging of peptide release from neuronal cells within microfluidic devices. Lab Chip. 2007; 7:1454–60. [PubMed: 17960271]

[11]. Wei HB, Li HF, Gao D, Lin JM. Multi-channel microfluidic devices combined with electrospray ionization quadrupole time-of-flight mass spectrometry applied to the monitoring of glutamate release from neuronal cells. Analyst. 2010; 135:2043–50. [PubMed: 20526497]

[12]. Yanik MF, Cinar H, Cinar HN, Chisholm AD, Jin YS, Ben-Yakar A. Neurosurgery - Functional regeneration after laser axotomy. Nature. 2004; 432:822. [PubMed: 15602545]

[13]. George EB, Schneider BF, Lasek RJ, Katz MJ. Axonal shortening and the mechanisms of axonal motility. Cell Motil. Cytoskeleton. 1988; 9:48–59. [PubMed: 2895686]

[14]. Erez H, Malkinso G, Pragel-Khoutorsky M, De Zeeuw CI, Hoogenraad CC, Spira ME. Formation of microtubule-based traps controls the sorting and concentration of vesicles to restricted sites of regenerating neurons after axotomy. J. Cell Biol. 2007; 176:497–507. [PubMed: 17283182]

[15]. Bedi SS, Glanzman DL. Axonal rejoining inhibits injury-induced long-term changes in *Aplysia* sensory neurons in vitro. J. Neurosci. 2001; 21:9667–77. [PubMed: 11739576]

[16]. Chang WC, Hawkes EA, Kliot M, Sretavan DW. In vivo use of a nanoknife for axon microsurgery. Neurosurgery. 2007; 61:683–91. [PubMed: 17986929]

[17]. Hosmane S, Fournier A, Wright R, Rajbhandari L, Siddique R, Yang IH, Ramesh KT, Venkatesan A, Thakor N. Valve-based microfluidic compression platform: Single axon injury and regrowth. Lab Chip. 2011; 11:3888–95. [PubMed: 21975691]

[18]. Kilinc D, Peyrin JM, Soubeyre V, Magnifico S, Saias L, Viovy JL, Brugg B. Wallerian-like degeneration of central neurons after synchronized and geometrically registered mass axotomy in a three-compartmental microfluidic chip. Neurotox Res. 2011; 19:149–61. [PubMed: 20162389]

[19]. Romanova EV, Oxley SP, Rubakhin SS, Bohn PW, Sweedler JV. Self-assembled monolayers of alkanethiols on gold modulate electrophysiological parameters and cellular morphology of cultured neurons. Biomaterials. 2006; 27:1665–69. [PubMed: 16197993]

[20]. Vanmali BH, Romanova EV, Messner MC, Singh M, Maruniak J, Sweedler J, Kirk MD. Endogenous neurotrophic factors enhance neurite growth by bag cell neurons of Aplysia. J. Neurobiol. 2003; 56:78–93. [PubMed: 12767034]

[21]. Romanova EV, Fosser KA, Rubakhin SS, Nuzzo RG, Sweedler JV. Engineering the morphology and electrophysiological parameters of cultured neurons by microfluidic surface patterning. FASEB J. 2004; 18:1267, 69. [PubMed: 15208266]

[22]. Sanchez AD, Li YS, Kirk MD. Regeneration of cerebral-buccal interneurons and recovery of ingestion buccal motor programs in *Aplysia* after CNS lesions. J. Neurophysiol. 2000; 84:2961–74. [PubMed: 11110824]

NIH-PA Author Manuscript

NIH-PA Author Manuscript

NIH-PA Author Manuscript

[23]. Prager-Khoutorsky M, Spira ME. Neurite retraction and regrowth regulated by membrane retrieval, membrane supply, and actin dynamics. Brain Res. 2009; 1251:65–79. [PubMed: 19022228]

[24]. Walters ET, Alizadeh H, Castro GA. Similar neuronal alterations induced by axonal injury and learning in. Aplysia Science. 1991; 253:797–99.

[25]. Bedi SS, Salim A, Chen SP, Glanzman DL. Long-term effects of axotomy on excitability and growth of isolated *Aplysia* sensory neurons in cell culture: Potential role of cAMP. J. Neurophysiol. 1998; 79:1371–83. [PubMed: 9497418]

[26]. Bedi SS, Cai DC, Glanzman DL. Effects of axotomy on cultured sensory neurons of *Aplysia*: Long-term injury-induced changes in excitability and morphology are mediated by different signaling pathways. J. Neurophysiol. 2008; 100:3209–24. [PubMed: 18842953]

[27]. Walters ET, Ambron RT. Long-term alterations induced by injury and by 5-HT in *Aplysia* sensory neurons: Convergent pathways and common signals. Trends Neurosci. 1995; 18:137–42. [PubMed: 7754525]

[28]. Baker M, Croll RP. Modulation of in vivo neuronal sprouting by serotonin in the adult CNS of the snail. Cell. Mol. Neurobiol. 1996; 16:561–76. [PubMed: 8956009]

[29]. Romanova EV, Roth MJ, Rubakhin SS, Jakubowski JA, Kelley WP, Kirk MD, Kelleher NL, Sweedler JV. Identification and characterization of homologues of vertebrate beta-thymosin in the marine mollusk. Aplysia californica J. Mass Spectrom. 2006; 41:1030–40.

[30]. Colby GP, Sung YJ, Ambron RT. mRNAs encoding the *Aplysia* homologues of fasciclin-I and beta-thymosin are expressed only in the second phase of nerve injury and are differentially segregated in axons regenerating in vitro and in vivo. J. Neurosci. Res. 2005; 82:484–98. [PubMed: 16237720]

[31]. Srivatsan M, Peretz B. Acetylcholinesterase promotes regeneration of neurites in cultured adult neurons of. Aplysia Neuroscience. 1997; 77:921–31.

[32]. Schacher S, Proshansky E. Neurite regeneration by *Aplysia* neurons in dissociated cell-culture: Modulation by *Aplysia* hemolymph and the presence of the initial axonal segment. J. Neurosci. 1983; 3:2403–13. [PubMed: 6655493]

[33]. Bransky A, Korin N, Levenberg S. Experimental and theoretical study of selective protein deposition using focused micro laminar flows. Biomed. Microdevices. 2008; 10:421–28. [PubMed: 18213521]

[34]. Meier M, Lucchetta EM, Ismagilov RF. Chemical stimulation of the *Arabidopsis thaliana* root using multi-laminar flow on a microfluidic chip. Lab Chip. 2010; 10:2147–53. [PubMed: 20544086]

[35]. Takayama S, Ostuni E, LeDuc P, Naruse K, Ingber DE, Whitesides GM. Laminar flows - Subcellular positioning of small molecules. Nature. 2001; 411:1016–16. [PubMed: 11429594]

[36]. Villa-Diaz LG, Torisawa YS, Uchida T, Ding J, Nogueira-De-Souza NC, O'Shea KS, Takayama S, Smith GD. Microfluidic culture of single human embryonic stem cell colonies. Lab Chip. 2009; 9:1749–55. [PubMed: 19495459]

[37]. Nie FQ, Yamada M, Kobayashi J, Yamato M, Kikuchi A, Okano T. On-chip cell migration assay using microfluidic channels. Biomaterials. 2007; 28:4017–22. [PubMed: 17583787]

[38]. Takayama S, Ostuni E, LeDuc P, Naruse K, Ingber DE, Whitesides GM. Selective chemical treatment of cellular microdomains using multiple laminar streams. Chem. Biol. 2003; 10:123–30. [PubMed: 12618184]

[39]. Bianchini A, Playle RC, Wood CM, Walsh PJ. Mechanism of acute silver toxicity in marine invertebrates. Aquat. Toxicol. 2005; 72:67–82. [PubMed: 15748748]

[40]. Tourovskaia A, Figueroa-Masot X, Folch A. Differentiation-on-a-chip: A microfluidic platform for long-term cell culture studies. Lab Chip. 2005; 5:14–19. [PubMed: 15616734]

[41]. Kupfermann. Stimulation of egg laying - possible neuroendocrine function of bag cells of abdominal ganglion of. Aplysia californica Nature. 1967; 216:814–15.

[42]. Chiu AY, Strumwasser F. An immunohistochemical study of the neuropeptidergic bag cells of. Aplysia J. Neurosci. 1981; 1:812–26.

NIH-PA Author Manuscript NIH-PA Author Manuscript NIH-PA Author Manuscript

[43]. Bhattacharya S, Datta A, Berg JM, Gangopadhyay S. Studies on surface wettability of poly(dimethyl) siloxane (PDMS) and glass under oxygen-plasma treatment and correlation with bond strength. J. Microelectromech. Syst. 2005; 14:590–97.

[44]. Shiku H, Saito T, Wu CC, Yasukawa T, Yokoo M, Abe H, Matsue T, Yamada H. Oxygen permeability of surface-modified poly(dimethylsiloxane) characterized by scanning electrochemical microscopy. Chem. Lett. 2006; 35:234–35.

[45]. Lambert JM. The nature of platinum in silicones for biomedical and healthcare use. J. Biomed. Mater. Res. Part B Appl. Biomater. 2006; 78B:167–80. [PubMed: 16470825]

[46]. Zhong M, Lee CY, Croushore CA, Sweedler JV. Label-free quantitation of peptide release from neurons in a microfluidic device with mass spectrometry imaging. Lab Chip. 2012; 12:2037–45. [PubMed: 22508372]

[47]. Lee JN, Park C, Whitesides GM. Solvent compatibility of poly(dimethylsiloxane)-based microfluidic devices. Anal. Chem. 2003; 75:6544–54. [PubMed: 14640726]

[48]. Sui GD, Wang JY, Lee CC, Lu WX, ee SP, Leyton JV, Wu AM, Tseng HR. Solution-phase surface modification in intact poly(dimethylsiloxane) microfluidic channels. Anal. Chem. 2006; 78:5543–51. [PubMed: 16878894]

[49]. Mehta G, Mehta K, Sud D, Song JW, Bersano-Begey T, Futai N, Heo YS, Mycek MA, Linderman JJ, Takayama S. Quantitative measurement and control of oxygen levels in microfluidic poly(dimethylsiloxane) bioreactors during cell culture. Biomed. Microdevices. 2007; 9:123–34. [PubMed: 17160707]

[50]. Walker GM, Zeringue HC, Beebe DJ. Microenvironment design considerations for cellular scale studies. Lab Chip. 2004; 4:91–97. [PubMed: 15052346]

[51]. Sugihara-Seki M. Flow around cells adhered to a microvessel wall. I. Fluid stresses and forces acting on the cells. Biorheology. 2000; 37:341–59. [PubMed: 11204541]

[52]. Dungan SR, Tai BH, Gerhardt NI. Transport mechanisms in the micellar solubilization of alkanes in oil-in-water emulsions. Colloids Surf. Physicochem. Eng. Aspects. 2003; 216:149–66.

[53]. Koley D, Bard AJ. Triton X-100 concentration effects on membrane permeability of a single HeLa cell by scanning electrochemical microscopy (SECM). Proc. Natl. Acad. Sci. U. S. A. 2010; 107:16783–87. [PubMed: 20837548]

[54]. Auborn JJ, Eyring EM, Choules GL. Kinetics of sodium dodecyl sulfate solubilization of *Mycoplasma laidlawii* plasma membranes. Proc. Natl. Acad. Sci. U. S. A. 1971; 68:1996–98. [PubMed: 5289357]

[55]. Siechen S, Yang SY, Chiba A, Saif T. Mechanical tension contributes to clustering of neurotransmitter vesicles at presynaptic terminals. Proc. Natl. Acad. Sci. U. S. A. 2009; 106:12611–16. [PubMed: 19620718]

[56]. Ahmed WW, Li TC, Rubakhin SS, Chiba A, Sweedler JV, Saif TA. Mechanical tension modulates local and global vesicle dynamics in neurons. Cell. Mol. Bioeng. 2012; 5:155–64. [PubMed: 23002399]

[57]. VanEssen DC. A tension-based theory of morphogenesis and compact wiring in the central nervous system. Nature. 1997; 385:313–18. [PubMed: 9002514]

[58]. Hanein Y, Tadmor O, Anava S, Ayali A. Neuronal soma migration Is determined by neurite tension. Neuroscience. 2011; 172:572–79. [PubMed: 20969931]

[59]. Lindsay RM. Nerve growth factors (NGF, BDNF) enhance axonal regeneration but are not required for survival of adult sensory neurons. J. Neurosci. 1988; 8:2394–405. [PubMed: 3249232]

[60]. Philp D, Badamchian M, Scheremeta B, Nguyen M, Goldstein AL, Kleinman HK. Thymosin beta 4 and a synthetic peptide containing its actin-binding domain promote dermal wound repair in db/db diabetic mice and in aged mice. Wound Repair Regen. 2003; 11:19–24. [PubMed: 12581423]

[61]. Bevelaqua FA, Kim KS, Kumarasiri MH, Schwartz JH. Isolation and characterization of acetylcholinesterase and other particulate proteins in hemolymph of. Aplysia californica J. Biol. Chem. 1975; 250:731–38.

[62]. Robertson RT. A morphogenic role for transiently expressed acetylcholinesterase in developing thalamocortical systems. Neurosci. Lett. 1987; 75:259, 64. [PubMed: 3587732]

NIH-PA Author Manuscript

NIH-PA Author Manuscript

NIH-PA Author Manuscript

[63]. Srivatsan M. An analysis of acetylcholinesterase sequence for predicting mechanisms of its non-catalytic actions. Bioinformation. 2006; 1:281–84. [PubMed: 17597908]

[64]. Schacher S, Rayport SG, Ambron RT. Giant *Aplysia* neuron R2 reliably forms strong chemical connections in vitro. J. Neurosci. 1985; 5:2851–56. [PubMed: 4056857]

[65]. He M, Zhang ZH, Guan CB, Xia D, Yuan XB. Leading tip drives soma translocation via forward F-actin flow during neuronal migration. J. Neurosci. 2010; 30:10885–98. [PubMed: 20702717]

[66]. Tan JL, Tien J, Pirone DM, Gray DS, Bhadriraju K, Chen CS. Cells lying on a bed of microneedles: An approach to isolate mechanical force. Proc. Natl. Acad. Sci. U. S. A. 2003; 100:1484–89. [PubMed: 12552122]

[67]. Hallstrom W, Lexholm M, Suyatin DB, Hammarin G, Hessman D, Samuelson L, Montelius L, Kanje M, Prinz CN. Fifteen-piconewton force detection from neural growth cones using nanowire arrays. Nano Lett. 2010; 10:782–87. [PubMed: 20102185]

[68]. Lamoureux P, Heidemann SR, Martzke NR, Miller KE. Growth and elongation within and along the axon. Dev Neurobiol. 2010; 70:135–49. [PubMed: 19950193]

[69]. Chan CE, Odde DJ. Traction dynamics of Filopodia on compliant substrates. Science. 2008; 322:1687–91. [PubMed: 19074349]

[70]. Difato F, Tsushima H, Pesce M, Benfenati F, Blau A, Chieregatti E. The formation of actin waves during regeneration after axonal lesion is enhanced by BDNF. Sci Rep-Uk. 2011; 1

[71]. Croushore CA, Supharoek SA, Lee CY, Jakmunee J, Sweedler JV. Microfluidic device for the selective chemical stimulation of neurons and characterization of Peptide release with mass spectrometry. Anal. Chem. 2012; 84:9446–52. [PubMed: 23004687]

[72]. Fan Y, Rubakhin SS, Sweedler JV. Collection of peptides released from single neurons with particle-embedded monolithic capillaries followed by detection with matrix-assisted laser desorption/ionization mass spectrometry. Anal. Chem. 2011; 83:9557–63. [PubMed: 22053721]

[73]. Rubakhin SS, Page JS, Monroe BR, Sweedler JV. Analysis of cellular release using capillary electrophoresis and matrix assisted laser desorption/ionization-time of flight-mass spectrometry. Electrophoresis. 2001; 22:3752–58. [PubMed: 11699914]

[74]. Nemes P, Knolhoff AM, Rubakhin SS, Sweedler JV. Metabolic differentiation of neuronal phenotypes by single-cell capillary electrophoresis-electrospray ionization-mass spectrometry. Anal. Chem. 2011; 83:6810–17. [PubMed: 21809850]

[75]. Kacharmina JE, Crino PB, Eberwine J. Preparation of cDNA from single cells and subcellular regions. Methods Enzymol. 1999; 303:3–18. [PubMed: 10349635]

NIH-PA Author Manuscript

NIH-PA Author Manuscript

NIH-PA Author Manuscript

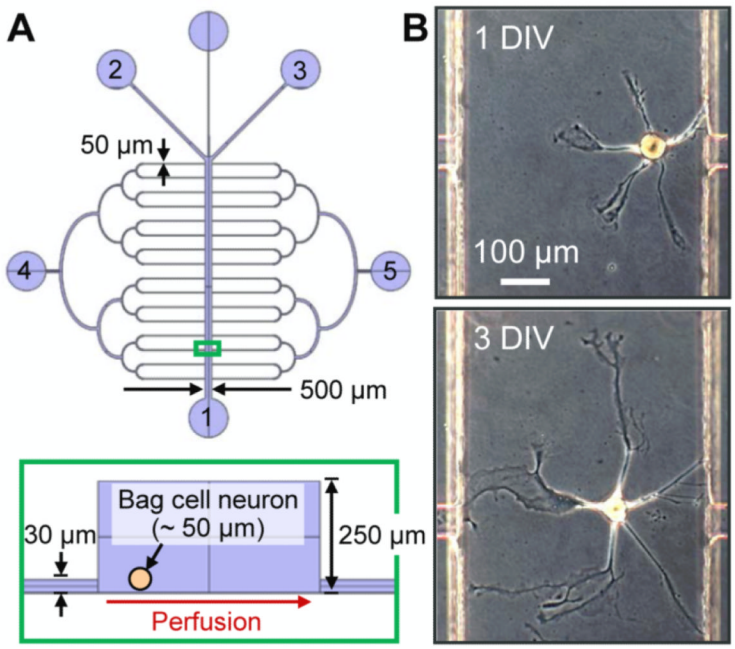

Figure 1.

Microfluidic device used for individual neuronal cell culture. **(A)** (*top*) Schematic of the device, which consists of a main channel for cell culture, side channels for media perfusion, and ports for fluidic connection; port 1 is an outlet during transection, ports 2 and 3 are for local delivery of SDS during transection, and 4 and 5 for media perfusion. (*bottom*) A cross-section of the selected region (green box) from the top image. **(B)** Bag cell neuron from *Aplysia californica* in the device (*top*) after 1 d *in vitro*, DIV, and (*bottom*) 3 DIV.

NIH-PA Author Manuscript

NIH-PA Author Manuscript

NIH-PA Author Manuscript

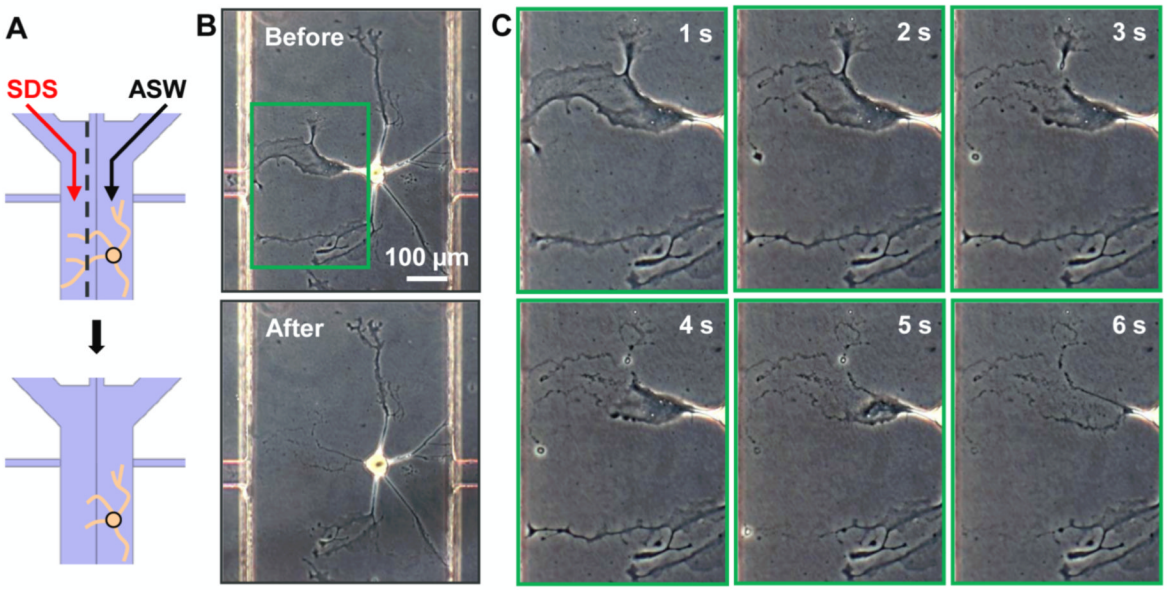

Figure 2.

A laminar stream of detergent is used for damaging (transecting) axons/neurites in a microchannel. **(A)** Schematic representation showing partial neurite damage of a single neuron. Using laminar flow, a stream of SDS is localized to the left portion of the channel to partially dissolve away the plasma membrane. The dotted line represents the boundary between SDS and ASW. **(B)** A bag cell neuron (*top*) before and (*bottom*) after transection. **(C)** Time-lapse images of the zoomed-in region (green box in B). The neurite damage upon exposure to SDS occurs within seconds.

NIH-PA Author Manuscript

NIH-PA Author Manuscript

NIH-PA Author Manuscript

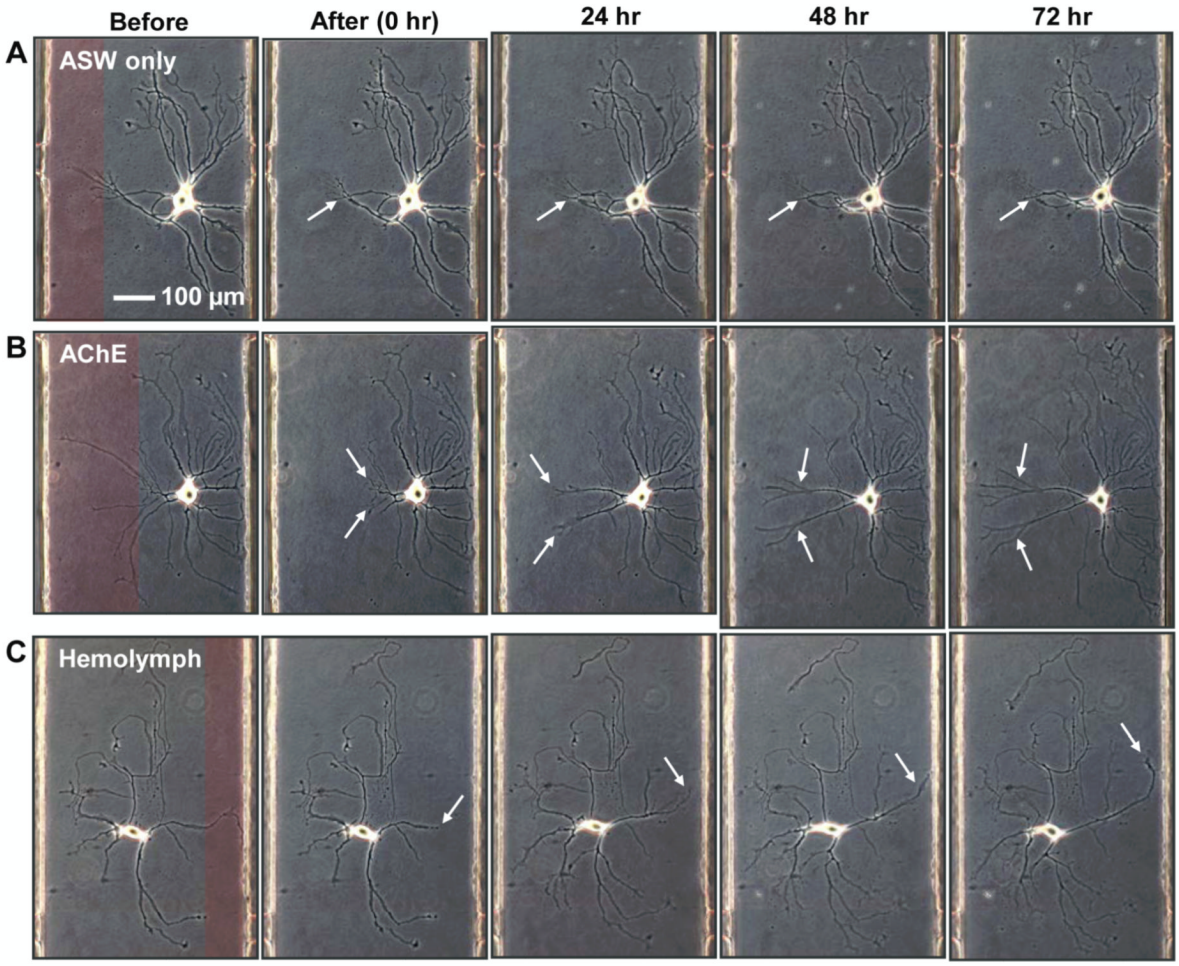

Figure 3.

The system aids in the study of neurotrophic factors effects on regeneration, here demonstrated using AChE and *Aplysia* hemolymph for bag cell neurons of *Aplysia*. Representative images of neurons are shown before and right after transection, and 24 h, 48 h, 72 h post-transection. Laminar streams of SDS are false-colored red in the first panels. Regeneration of the damaged neurites is minimal when the culture is maintained in **(A)** ASW only, whereas the process is greatly enhanced by supplementing the media with **(B)** (AChE) or **(C)** *Aplysia* hemolymph during regeneration. White arrows indicate the neurites damaged and regenerating.

NIH-PA Author Manuscript

NIH-PA Author Manuscript

NIH-PA Author Manuscript

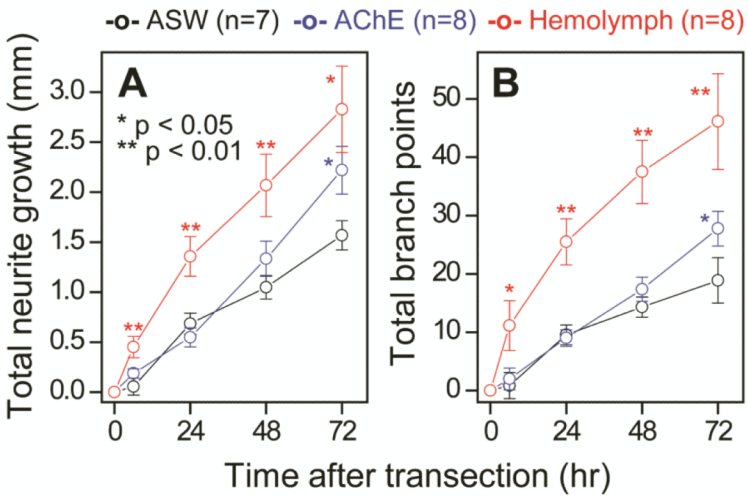

Figure 4.

Quantitative analysis of neurites verifies that AChE and *Aplysia* hemolymph help the regeneration of damaged bag cell neurons. Graphs show **(A)** the total length of fresh neurites and **(B)** the total number of new branch points after transection in ASW only (black), AChE (blue), and hemolymph (red). Compared to the neurons cultured in ASW only, those in AChE and hemolymph-supplemented media regenerate faster, with their neurites more branched. Error bars indicate standard error of the mean.

NIH-PA Author Manuscript

NIH-PA Author Manuscript

NIH-PA Author Manuscript

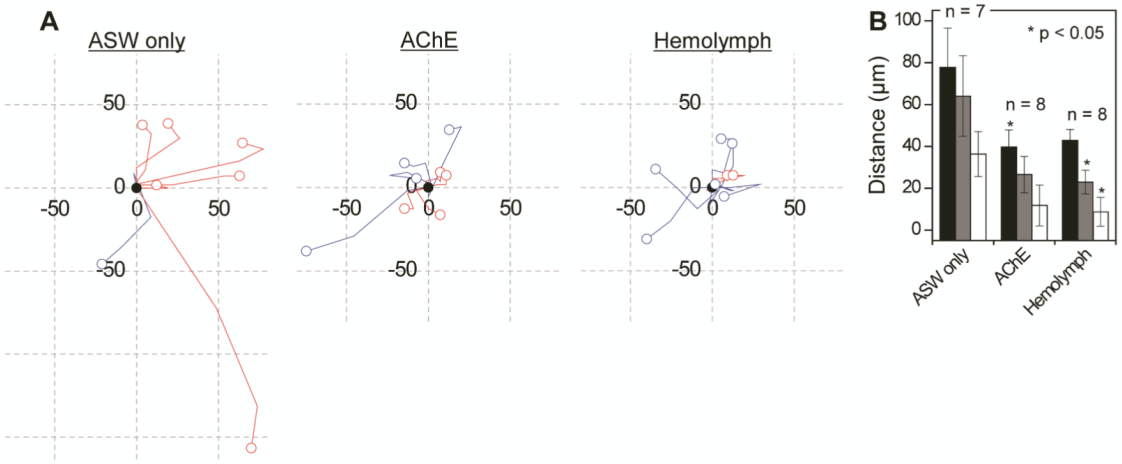

Figure 5.

During neuronal regeneration the migration of soma is suppressed when appropriate neurotrophic factors are present. **(A)** The paths of somata migration from 0 h (black filled circles) to 72 h after the transection (open circles) for the cells in (*left*) ASW only, (*middle*) AChE, and (*right*) hemolymph. Cells with neurite damage on the left- and right-hand side of the soma are colored red and blue, respectively. A grid cell indicates 50 μm × 50 μm. **(B)** A bar chart showing the total migration distance (black), the overall linear displacement (gray), and the x-direction displacement away from the injury site (white) of cell bodies at 72 h post-transection. Error bars indicate standard error of the mean.